

Evaluation of different methods for deriving geotechnical parameters from electric and seismic streamer data

Original

Evaluation of different methods for deriving geotechnical parameters from electric and seismic streamer data / Vagnon, Federico; Comina, Cesare; Arato, Alessandro. - In: ENGINEERING GEOLOGY. - ISSN 0013-7952. - 303:(2022), p. 106670. [10.1016/j.enggeo.2022.106670]

Availability:

This version is available at: 11583/2961726 since: 2022-04-21T09:03:23Z

Publisher:

Elsevier

Published

DOI:10.1016/j.enggeo.2022.106670

Terms of use:

This article is made available under terms and conditions as specified in the corresponding bibliographic description in the repository

Publisher copyright

Elsevier postprint/Author's Accepted Manuscript

© 2022. This manuscript version is made available under the CC-BY-NC-ND 4.0 license
<http://creativecommons.org/licenses/by-nc-nd/4.0/>. The final authenticated version is available online at:
<http://dx.doi.org/10.1016/j.enggeo.2022.106670>

(Article begins on next page)

Evaluation of different methods for deriving geotechnical parameters from electric and seismic streamer data.

Vagnon Federico^{1,2*}, Comina Cesare¹, Arato Alessandro³

¹ University of Torino, Department of Earth Sciences, 10125, Torino, Italy
federico.vagnon@polito.it; cesare.comina@unito.it

¹ Politecnico di Torino, Department of Environment, Land and Infrastructure Engineering,
10129, Torino, Italy

³ Techgea S.r.L, 10137, Torino, Italy
arato@techgea.eu

*corresponding author

Abstract

Geotechnical parameters of linear earth structures, such as embankments and earth dams, are usually obtained from point-wise investigations through drilling or penetration tests, commonly time and cost consuming. Non-invasive geophysical investigations may be considered alternative for a preliminary screening of earth structures physical properties, given their surveying speed and their depth and length of investigation. Seismic and electrical methods can be also used, through specific correlations, for the estimation of geotechnical soil characteristics. Several methodologies have been developed over the years combining two or more geophysical techniques for the estimation of geotechnical parameters.

In this paper, three different methods (with theoretical, statistical, and field based approaches respectively) for geotechnical parameters estimation from integrated geophysical surveys were compared, highlighting their strongpoints and limitations also by comparison with available direct geotechnical investigations.

Integrated seismic and electrical data from extensive surveying performed over seven retaining structures located in Piedmont Region (NW Italy) were used to forecast their fine content and hydraulic conductivity distributions. Geophysical data were acquired using seismic and electric streamers, useful for the simultaneous execution of the surveys in motion along the earth structures. The results of this study show the effectiveness of the proposed data acquisition approach and elaboration procedures as a first screening tool for earth retaining structure safety assessment. The increased capability of the theoretical method to better predict geotechnical parameters with respect to the other methodologies is also reported.

Article Highlights:

- different methods for geotechnical parameters estimation from integrated seismic and electrical geophysical surveys were compared;
- data from extensive surveying performed over seven retaining structures in Piedmont Region (NW Italy) were used to forecast fine content and hydraulic conductivity distributions;
- strongpoints and limitations of the proposed approaches in the aim of a first screening tool for earth retaining structure safety assessment are discussed.

Keywords: River embankment, Earth dam, Seismic and electric methods, Geotechnical investigations.

1. Introduction

Embankments and earth dams are engineering structures constructed for water supply, energy production or for water flow control in rivers and streams. Their stability and integrity evaluations are an important geotechnical problem for their safety assessment and the prevention from floods and dam-break related risk. Indeed, in the last five decades, these adverse phenomena have generated worldwide significant economic and human losses ([Hoyois and Sapir 2003](#)). The reported number of disasters caused by floods has dramatically increased because of climate changes and aging of most of the retaining structures.

Stability and integrity of these structures can be compromised by cyclic hydraulic gradients, causing seepage, internal erosion and piping especially when: i) the foundation materials are not sufficiently compacted, ii) heterogeneities are present in the embankment body or iii) the natural aging of the embankment has affected the integrity of some isolated portions. Moreover, localized invasive wildlife activities may negatively affect their hydraulic performances and their structural integrity with burrows excavated in the main embankment body or at the contact with foundation soil. All these phenomena reflect in relevant variations in the geotechnical parameters that need to be properly characterized for assessing the state of health of the structure. Moreover, in correspondence with intense rainfall events, which cause relevant hydraulic gradient variations, the timing of the characterization campaigns can be an important aspect to consider.

Consequently, rapid and reliable characterization tools are required for the identification of localized anomalies within the structure bodies. Conventional geotechnical methods for the characterisation involve invasive techniques such as borings (with sample collection for detailed laboratory tests) and penetration tests. These methodologies provide local detailed information of the structure layering but are affected by three main limitations: i) they provide only punctual data and are not sensitive to lateral heterogeneities, ii) they are expensive and iii) time-consuming.

On the other hand, non-invasive geophysical techniques allow nearly continuous determination of physical properties that can be helpful in location of anomalies and safety assessment. Given the significant linear extension of protection structures and the localized nature of weakness points, these techniques may be considered a good compromise between the surveying speed, the depth and length of investigation and reliability of the results.

Since the soil layering, the variation in water content and the hydraulic conditions have a great influence on the probability of global and local failure, the application of electrical resistivity methods (e.g. Electrical Resistivity Tomography, ERT) and surface wave tests (e.g. Multichannel Analysis of Surface Wave, MASW) are useful tools for linear earth structure characterization. Several applications of these methodologies can be found in literature (e.g. [Al-Fares 2014](#), [Arosio et al. 2017](#), [Camarero et al. 2019](#), [Cardarelli et al. 2014](#), [Chen et al. 2006](#), [Comina et al. 2020a](#), [Comina et al. 2020b](#), [Goff et al. 2015](#), [Hayashi et al. 2013](#), [Takahashi et al. 2014](#), [Weller et al. 2014](#), [Rittgers et al. 2016](#)). In recent years, the use of mobile geoelectric and seismic systems for a preliminary characterization along river embankment has indeed risen ([Brown et al. 2011](#), [Comina et al. 2020a](#), [Comina et al. 2020b](#), [Dabas, 2011](#), [De Domenico et al. 2016](#), [Kuras et al. 2007](#), [Sorensen 1996](#), [Vagnon et al. 2021](#)) due to their flexibility and increased surveying speed.

In complex geotechnical and hydraulic conditions, and possibly with presence of artefacts (such as metallic diaphragms or drainage pipes), a single geophysical method may lead to misinterpretations. Indeed, ERTs alone cannot distinguish whether low resistivity sectors are due

to high water content or clay soil or a buried conduit. Conversely, velocity reductions evidenced by MASW could be associated both to an increase of soil fine fraction content or to an increase of the saturation degree or soil plasticity.

Integrated geophysical approaches, combining shear wave velocity (V_s) and resistivity (R), can therefore provide a more accurate description of soil type than the individual methodologies alone (Hayashi et al. 2013). In addition, several researchers have developed theoretical, statistical, or field-based methods for specific geotechnical parameters estimation (soil type, fine fraction content, porosity, hydraulic conditions) from integrated geophysical surveys (Arato et al. 2021, Brovelli and Cassiani 2010, Carcione et al. 2007, Chen et al. 2006, Cosentini and Foti 2014, Glover et al. 2000, Goff et al. 2005, Hashin and Shtrikman 1963, Hayashi et al. 2013, Takahashi et al. 2014).

In this framework, the present paper report on extensive surveying performed over seven retaining structures located in Piedmont Region (NW Italy) by means of combined ERT and MASW surveys. Both R and V_s data were acquired over the retaining structures by means of appropriate streamers developed for these specific investigations. The geophysical data were used for detecting localized anomalies and estimating the geotechnical parameters with three different methodologies available in literature. Strongpoints and limitation of these methodologies are highlighted and discussed also in comparison with available independent geotechnical data over the same structures.

2. Case studies and data acquisition

Seismic and electric data were collected over seven earth retaining structures located in Piedmont Region (NW Italy): five river embankments (Bormida, Chisola DX and SX, Maira and Moncalieri) and two small earth dams (Arignano and Briaglia). Their geographical location is shown in Fig. 1 and their main characteristics are summarized in Table 1 and Fig. 2.

These case studies were selected following three main criteria: i) availability of independent geotechnical investigations for comparing and validating geophysical results, ii) coverage of a wide range of construction materials, iii) representativeness of a wide range of structure characteristics. Regarding the last point, the analyzed sites cover different earth retaining structure typologies, characterized by different pathologies. There are two embankments characterized by known anomalies, due to animal burrows (Moncalieri) and rupture restoration works (Chisola SX), one historical embankment subjected to aging phenomena and repeatedly repaired during the time (Bormida), one embankment characterized by a potential seepage phenomenon due to the stress of several flood events (Chisola DX) and one newly built (Maira) but already showing localized instabilities. Finally, two small earth dams were also selected: a historical one with the presence of a brick channel that cross the main body (Arignano) and one built in the 1990s (Briaglia) and affected by aging phenomena.

Fig. 2 shows the ternary plot of the average grain size distributions for the embankment bodies and the foundation soils. These data come from point-wise geotechnical investigations performed on each analysed case study: consequently, they refer to an average soil layering and local lateral variations are neglected. As a general comment, embankment bodies are usually made by finer soils (mainly silt and clay with lower percentage of sand) compared to the foundation soils that are generally composed by fluvial deposits with high percentage of gravel and sand and potential presence of rock boulders. The differences between the properties of the main body and foundation soils in earth dams are conversely less marked, especially in the shallow portions (Fig. 2b Arignano and Briaglia markers). A short description of the tested sites is reported in the following.

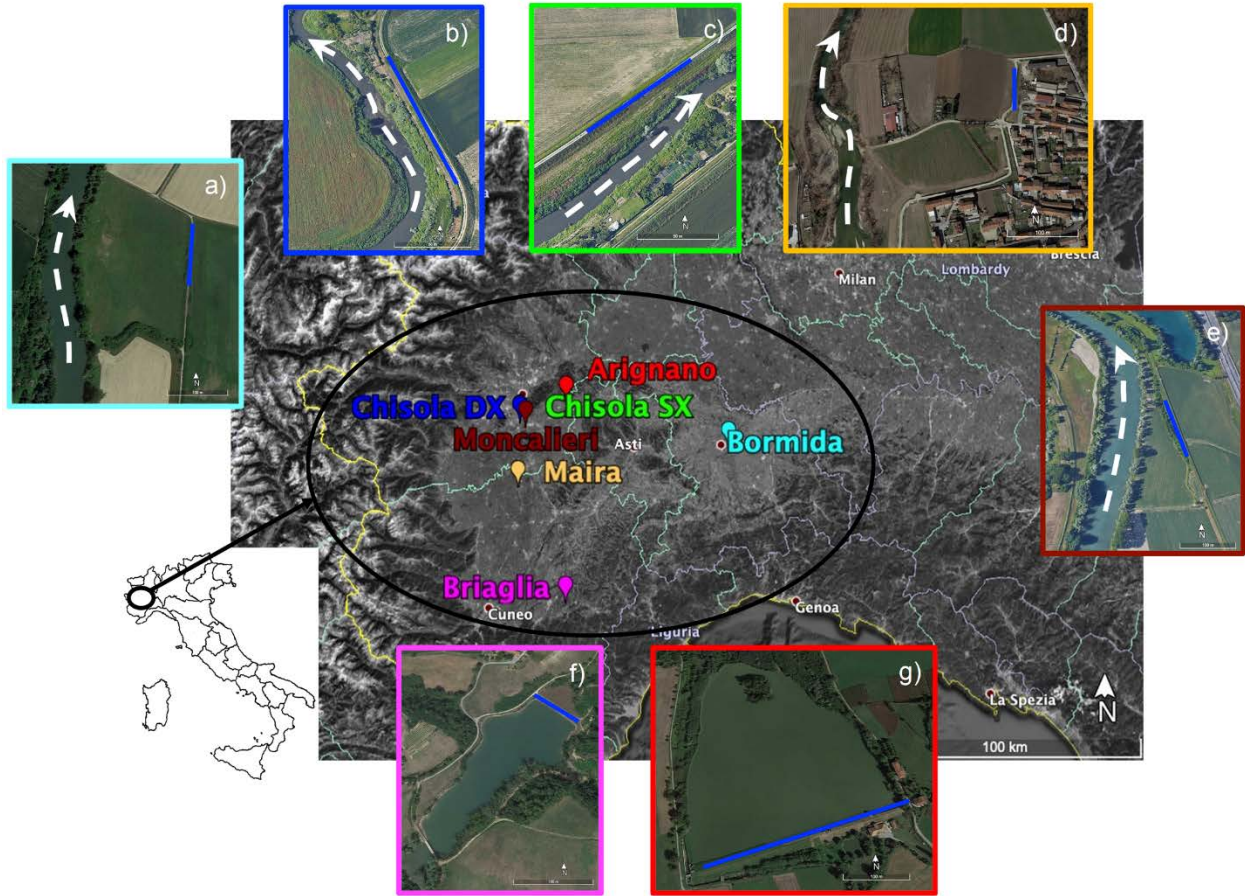


Figure 1. Location of the case studies in Piedmont Region (NW Italy): a) Bormida, b) Chisola DX, c) Chisola SX, d) Maira and e) Mocalieri embankments, f) Arignano and g) Briaglia earth dams. Blue continuous lines and white dashed arrows respectively represent the geophysical surveys and the river flow directions.

Table 1. Summary of main characteristic of the considered case studies.

Site	Retaining structure type	Average main body height [m]	Survey length [m]	Structural pathologies or potential instability warnings
Bormida	Embankment	5	90	Aging
Chisola DX	Embankment	2.5	114	Stressed by numerous flood events with potential seepage
Chisola SX	Embankment	4	110	Restored after recent flood event
Maira	Embankment	2	76	Newly built with local shallow instabilities
Moncalieri	Embankment	3	126	Presence of localized burrows from wildlife activities
Arignano	Earth dam	8	278	Aging and presence of a brick channel in the main body
Briaglia	Earth dam	11	72	Aging

Bormida River embankment

The right embankment of the Bormida River (44°53'51.16"N, 8°38'46.53"E, Fig. 1a), rises about 7 m from the free surface of the river, and about 3 m from the surrounding floodplain. The embankment was repeatedly repaired over years after several flood events that caused local ruptures and instabilities. The soil composition of the embankment consists of silt with fine sand within the first embankment layer and fine to medium-grained sand at the interface with the foundation soil. The latter is mainly made of sand and gravel (Fig. 2).

2.1 Chisola DX and SX embankments

The right (DX) and left (SX) embankments of the Chisola River (44°58'43.83"N, 7°40'32.17"E, Fig. 1b and 1c respectively) have a trapezoidal shape with an average height of about 3 m above ground level, a width of about 9 m at the base and of about 4 m at the top. These embankments have been stressed by various flood events during the years, due to intense precipitations and consequent rise of water levels. In the latest event, in November 2016, a localized rupture (about 40 m in length) of the left embankment (Chisola SX) occurred, and restoration works were undertaken to seal and repair the embankment. The reconstructed sector of the embankment is mainly constituted of clay and silt, while the surrounding portions and the foundation soils have a high percentage of sand (Fig. 2). The right embankment (Chisola DX) is constituted by natural silty and sandy alluvial deposits taken from the surrounding plain. This embankment was not specifically damaged by previous flood events but, given the damage of the corresponding Chisola SX embankment, the risk of seepage may be hypothesised high.

2.2 Maira River embankment

The Maira River embankment (44°46'13.79"N, 7°40'12.48"E, Fig. 1d) is a shallow (about 2 m) newly built embankment to protect the city of Racconigi. This embankment was constructed with selected uniform clayey material directly on the alluvial plain deposits constituted of gravelly sand (Fig. 2). The embankment experienced some landslips along the slopes, caused by the transit of heavy trucks and excavators on the crest road.

2.3 Po River (Moncalieri) embankment

The Po River embankment (named here Moncalieri, 44°57'50.48"N, 7°42'7.37"E, Fig. 1e) is 2 m high and was built in the early 20th century to protect the main highway from Torino towards the south. It is built with alluvial sediments (silty sands, Fig. 2) probably exploited from surrounding caves or directly from river deposits. Along this embankment, several badger burrows were detected and considered responsible of several small instabilities.

2.4 Arignano dam

The Arignano earth dam (45° 2'40.91"N, 7°53'26.85"E, Fig. 1f) was built at the beginning of 1800s as a water supply reservoir for agricultural purposes. The dam has a trapezoidal shape, with longitudinal extension of about 380 m, maximum height of 8 m and width, at the base, of about 60 m, and at the toe of about 4 m.

The dam body is mostly made of silt and clay (Fig. 2) and it is founded directly on the natural alluvial soil. The peculiarity of this structure is the presence of a brick channel within the dam body, used in the past for powering the mill located downstream of the dam. This channel, 2 m wide, 1.5 m tall and approximately 20 m long, has warned the authorities on the possibility of inducing preferential seepages and local instabilities.

2.5 Briaglia dam

The Briaglia dam (44°24'10.02"N, 7°53'33.21"E, Fig. 1g) was built at the beginning of 1990s as a water supply reservoir for agricultural purposes. It has a trapezoidal shape with a spillway and adequate rockfill on the upstream to protect the dam from the wave flux. The dam has a total length of about 90 m and a maximum height of about 11 m. The dam body composition varies, from the embankment crest to the foundation soil interface, between medium-dense sandy silt to silty-clayey sand. The foundation soil is composed of stiff clay and stiff clayey marl (Fig. 2). The dam has been monitored in the last years to detect possible aging-related degradation of its geotechnical performance.

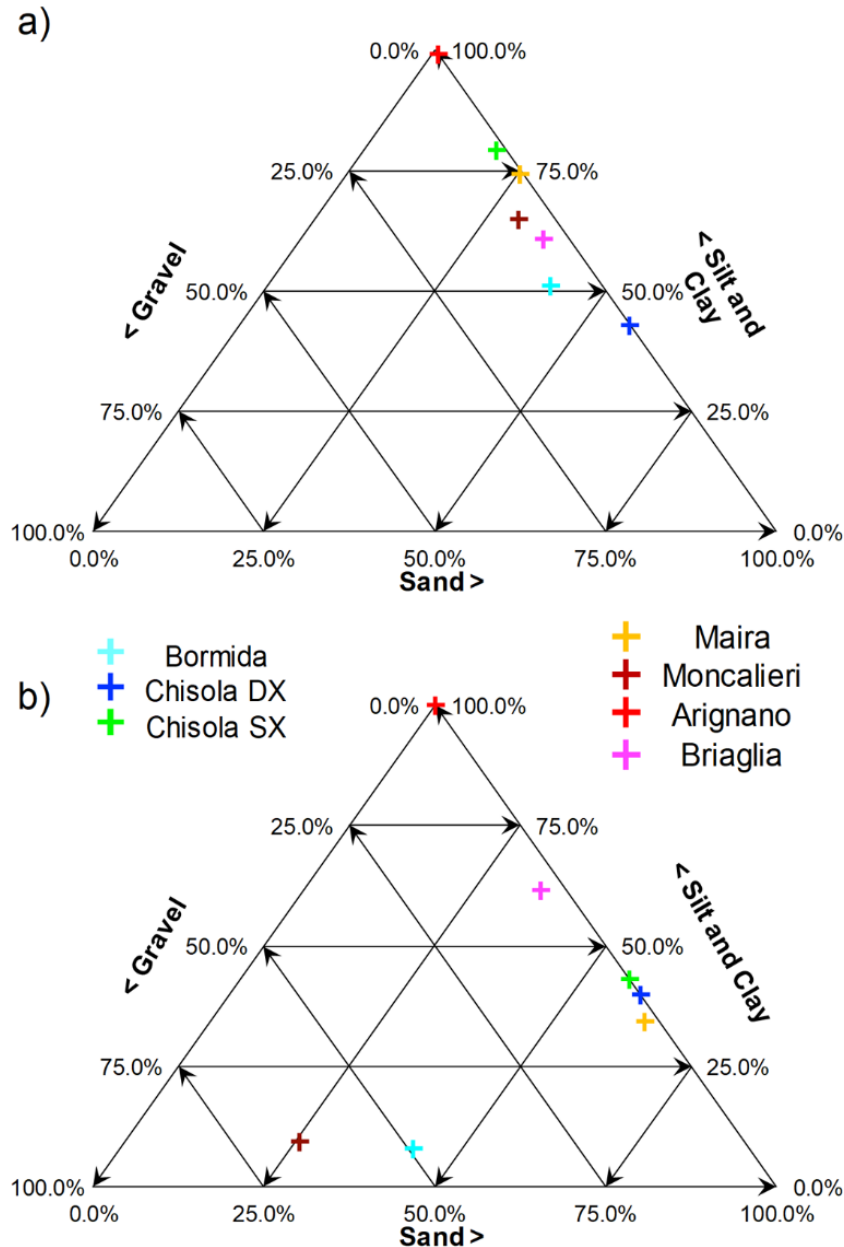


Figure 2. Ternary plots of the average grain size distributions for a) the embankment bodies and b) the foundation soils, for each analysed case study.

2.6 Resistivity and shear wave velocity surveys

The surveys over the investigated sites were performed using two different streamers dragged by a vehicle on the top of the retaining structures with data recording at 2 m steps (Fig. 3). For each step, one electric sequence and a single seismic shot were acquired. The data were referred to the respective streamer mid-points and used for integrated interpretation at the same positions. The total survey lengths for each case study are reported in Tab. 1.

The electric streamer consists of 12 electrodes, that can be used both as current and potential electrodes, symmetrically spaced around the streamer mid-point, with a total length of 46 m. The measurement sequence was based on Wenner-Schlumberger and Dipole-Dipole quadrupoles. The electrodes were connected to the acquisition system (Syscal-Pro, Iris Instruments, georesistivimeter), stored on the vehicle, by means of a multipolar cable. For the seismic surveys, an array of 24, 4.5 Hz vertical geophones 1 m spaced was deployed aside to the geoelectrical one and dragged by the same vehicle. A 40 kg accelerated mass was used as a seismic source and located with a 6 m offset from the first geophone. Seismograms were acquired by a DAQ-Link IV seismograph (Seismic Source) with a 0.5 ms sampling interval, -50 ms pretrig and 1.024 s total recording length.

Both electric and seismic acquisitions guaranteed a dense data coverage and a maximum depth of investigation (DOI) of about 10 m (actually the seismic survey DOI is deeper, see [Comina et al. 2020b](#)), which is satisfactory for investigating the dam/embankment body and the first meters of foundation soil where the main instability phenomena may occur.

Seismic and electric data were post-processed in office: the electric data were filtered and inverted with the commercial code Res2DInv ([Loke and Barker 1996](#)) while the seismic data were analyzed with a specific procedure for the analysis of Rayleigh wave fundamental mode dispersion curves (DC). Further details on the acquisition system and data processing can be found in [Comina et al. \(2020a, 2020b\)](#).

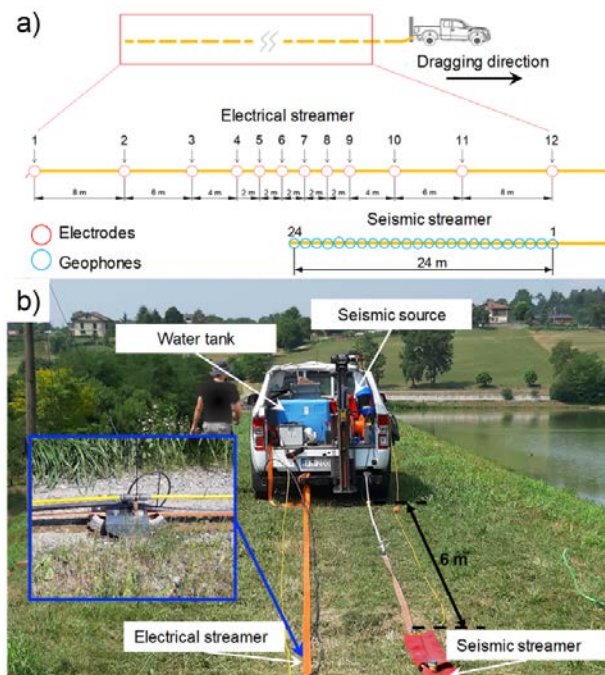


Figure 3. a) Scheme of the electrical and seismic streamers adopted for the characterization. b) Details of the seismic source and acquisition systems.

3. Methodology

In this section, three methods for the estimation of geotechnical parameters from integrated geophysical data will be analysed. The methods are representative of the main approaches developed for the characterization of earth linear structures with geophysical data: theoretical, statistical and field-based approaches. All the three methods have been later applied to the acquired field data in order to highlight strong points, shortcomings, and possible discrepancies between predicted results and field evidence.

3.1 Theoretical approach

Takahashi et al. (2014), and later Vagnon et al. (2021), developed an integrated method for profiling soil permeability of river embankments by coupling seismic and electric data. The clay content of the soil, C , (assumed as the fine soil fraction i.e. both silt and clay) can be defined from combined geophysical data by superimposing the experimental electrical resistivity, R , and shear wave velocity, V_s , values from field measurement to theoretical constant C curves and finding the nearest C curve to which they can be associated. The theoretical C curves can be derived from the theoretical V_s -porosity and R -porosity trends, defined from the Glover's model (Glover et al. 2000), the Hashin-Shtrikman upper bound model (Hashin and Shtrikman 1963) and the Voigt-Reuss-Hill model (Mavko et al. 2009).

In detail, the Glover's model expresses the relationship between formation resistivity, R , and porosity, ϕ , as follows:

$$\frac{1}{R} = \frac{1}{R_s} (1 - \phi)^{\frac{\log(1-\phi^m)}{\log(1-\phi)}} + \frac{1}{R_f} \phi^m S_w^q \quad (1)$$

where R_s and R_f are the soil grains and fluid resistivities respectively, m is the cementation factor, q is the saturation index and S_w is the saturation degree.

The soil grain resistivity, R_s , can be express as a function of the resistivity of the fine soil fraction (R_{clay}) and its content, C , by using the Hashin-Shtrikman upper bound model:

$$\frac{1}{R_s} = \frac{1}{R_{clay}} \left[1 - \frac{3(1-C)\Delta R}{\frac{3}{R_{clay}} - C\Delta R} \right] \quad (2)$$

with ΔR being the difference between the electrical conductivity of the soil fine fraction, $1/R_{clay}$, and the one of the sand fraction, $1/R_{sand}$, i.e. $\Delta R = \frac{1}{R_{clay}} - \frac{1}{R_{sand}}$.

The theoretical relationship between V_s and porosity is evaluated by combining the Hashin-Shtrikman lower bound and the Voigt-Reuss-Hill model as follows:

$$V_s = \sqrt{\frac{\left(\left(\frac{\phi}{\phi_0} + \frac{1-\phi}{\phi_0} \right)^{-1} - Z \right)}{\rho}} \quad (3)$$

with:

$$Z = \frac{G_{HM}}{6} \cdot \frac{9K_{HM} + 8G_{HM}}{K_{HM} + 2G_{HM}} \quad (4)$$

$$K_{HM} = \left[\frac{n^2(1-\phi)^2 G_g^2}{18\pi^2(1-\nu)^2} P \right]^{\frac{1}{3}} \quad (5)$$

$$G_{HM} = \left[\frac{5-4\nu}{5(2-\nu)} \right] \left[\frac{3n^2(1-\phi)^2 G_g^2}{2\pi^2(1-\nu)^2} P \right]^{\frac{1}{3}} \quad (6)$$

$$G_g = \frac{(1-C)G_{sand} + CG_{clay} + \left(\frac{1-C}{G_{sand}} + \frac{C}{G_{clay}} \right)^{-1}}{2} \quad (7)$$

and where ρ is the bulk density of the soil, G_{HM} and K_{HM} are respectively the shear and bulk moduli of the soil at the critical porosity, ϕ_0 , in the Hertz-Mindlin model (Mavko et al. 2009), n is the coordination number, P is the confining pressure, ν is the Poisson's ratio of the soil, G_{sand} and G_{clay} are respectively the shear moduli of sand and clay components, and G_g is the shear modulus of the soil grains.

These parameters can be assumed based on the wide scientific literature on this topic.

Once the clay content has been obtained, the porosity can be obtained by inverting Equation 1 and R-porosity and Vs-porosity relations can be used for estimating R-Vs relation. The latter can be used to estimate the average grain size, d . The hydraulic conductivity can then be calculated by using Kozeny-Carman relation (Carman 1956):

$$K = 9.8 \cdot 10^6 \cdot \frac{1}{72} \cdot \frac{\phi^3}{(1-\phi)^2 \cdot (1-\ln(\phi^2))} \cdot d^2 \quad (8)$$

Many assumptions are required for the application of this formulation, particularly the value of the clay fraction resistivity, R_{clay} , which has to be calibrated as a function of the specific mineralogy and cation exchange capacity of the clay present at the embankment site. Conversely, the fluid resistivity, R_f , is usually available or can be easily measured independently from samples of the surrounding water. If specifically calibrated with borehole data, this methodology has proven its effectiveness and reliability in profiling earth retaining structures (Takahashi et al. 2014, Vagnon et al. 2021).

3.2 Statistical approach

Hayashi et al. (2013) proposed a polynomial approximation for the estimation of soil parameters, such as fine fraction content (F_c), 20% average grain size (D_{20}), blow counts from standard penetration tests (N_{SPT}) and soil types, by using the cross-plots of shear wave velocity and resistivity.

They collected the results of geophysical surveys performed over 37 Japanese embankments, for a total length of 600 km and correlated them with 400 km of borings. Retaining structures soil was classified into clay, sand and gravel: further distinction was made between foundation soil and embankment body.

The following equation was proposed for the estimation of soil parameters:

$$S_i = aV_s^2 + bV_s + c(\log_{10} R)^2 + d \log_{10} R + eV_s^2 \log_{10} R + fV_s(\log_{10} R)^2 + gV_s \log_{10} R + h \quad (9)$$

where S_i is the considered soil parameter (F_c , D_{20} , N_{SPT} and soil type) and a to h are the polynomial coefficients available in Hayashi et al. (2013). These latter were obtained by minimizing the differences between each S_i and the soil parameters obtained from independent geotechnical surveys through a least squares optimization. This formulation is therefore purely empirical, and it is not certain how it can be applied to a broad type of soils.

3.3 Field-based approach

Chen et al. (2006) developed a seepage index (F) for assessing potential seepage in the Laocheng embankment (Songzi County, Hubei Province, China) by combining results from surface-wave tests and electric resistivity measurements. F is a dimensionless index defined as:

$$F = \frac{k_S}{V_S} + \frac{k_R}{R} \quad (10)$$

where k_S and k_R are empirical coefficients in m/s and Ωm respectively. The index F has both a theoretical and field-based origin. Usually, lower resistivity and shear wave velocity values are correlated with higher moisture content. Moreover, lower shear wave velocity indicates soft soils. Consequently, higher F -values can indicate excessive seepage or piping phenomena.

The values of k_S and k_R were calibrated from seismic and electric measurements and on-site characteristics. Indeed, by superimposing V_S and R data on locations where seepage and piping occurred, Chen et al. (2006) observed that F assumed values greater than 2. Consequently, k_S and k_R coefficients were back calculated and set respectively equal to 80 m/s and 5 Ωm . Since their selection is not unique, the authors suggested to determine them by background values (or average values) of shear wave velocity and resistivity through the entire dataset if no drilling data were available. Alternatively, selection of coefficients may be done by comparing with measured V_S and R around seepage areas if such data exist.

In this paper, F and k values were compared and the highlighted differences were analysed and discussed with coefficients and soil parameters calibrated on each case study.

4. Results

Results of geophysical surveys are shown in Fig. 4. For each case study, V_S - R values along the retaining structures (circle markers) and median values (cross markers) are reported both for the embankment body (Fig. 4a) and for the foundation soil (Fig. 4b). The shift directions between median V_S - R values of embankment body and foundation soils for each analysed structure are also reported (Fig. 4c). For all the investigated structures the constituting soil of the embankment bodies show lower resistivity values than foundation soil (Fig. 4c). These differences are however reduced in some cases (i.e. Arignano, Chisola SX and Moncalieri) due to the reduced contrast among embankment body and foundation soil. In the Arignano and Chisola SX case studies this reduced contrast reflect in a moderate decrease in V_S from embankment body to foundation soil. In all the other structures an increase in V_S from embankment body to foundation soil is observed. This increase is more marked in the Briaglia dam due to the higher stiffness of the constituting foundation soil (stiff clay).

At a first sight by analysing Figs 2 and 4, a good correspondence between average grain size distributions and median V_S - R values can be deduced. Generally, by increasing the sand and gravel content of both embankment body and foundation soil, both resistivity and seismic velocity values increase. Indeed the evidenced shifts to higher R values from embankment body to foundation soils (Fig. 4c) is reflected in an increase in sand and gravel content (Fig. 2 a to b). Moreover, the

magnitude of the resistivity shift appears proportional to the contrast between the embankment body and foundation soils.

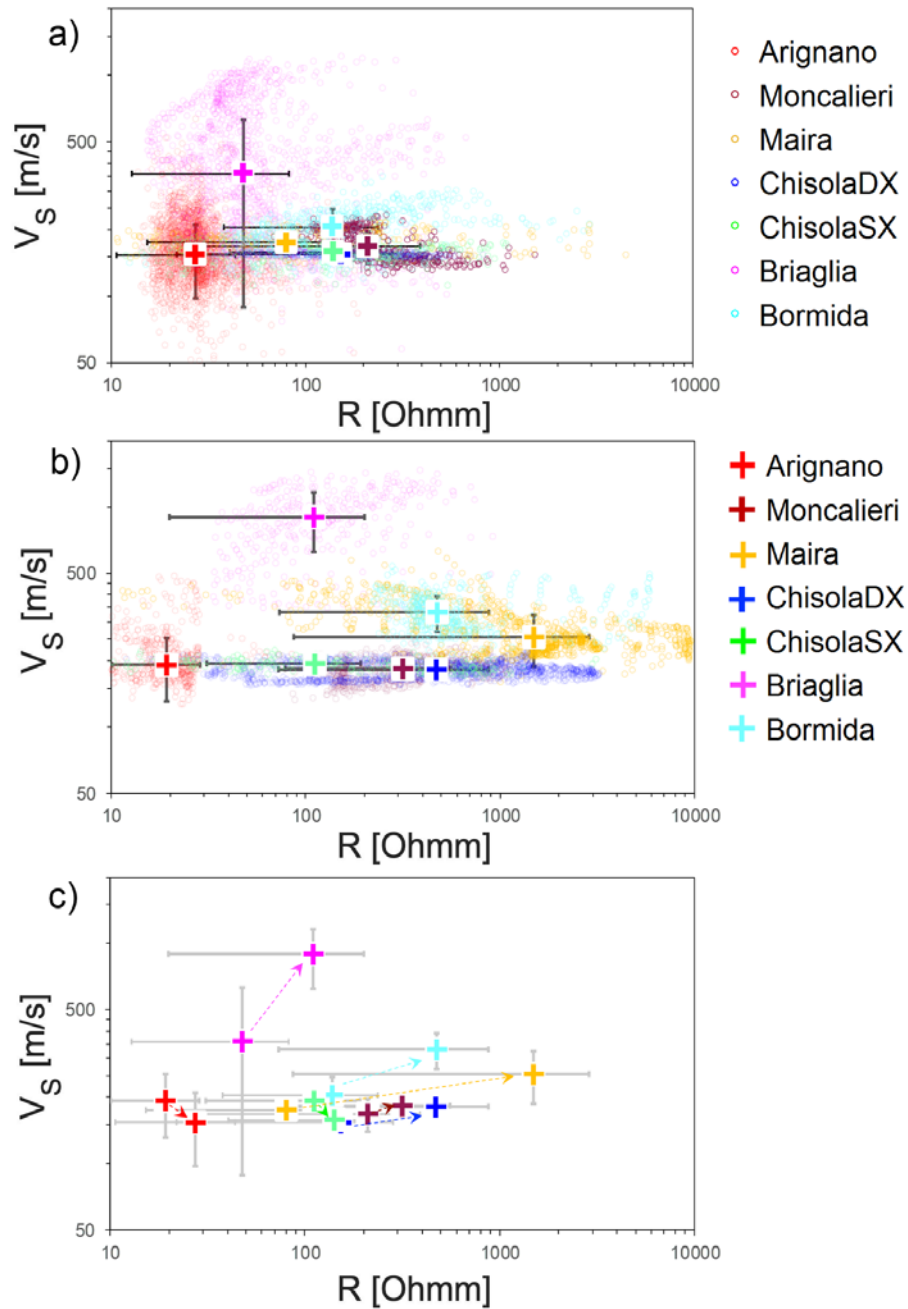


Figure 4. Distribution of the measured electrical resistivity (R) and shear wave velocity (V_s) values (coloured circles) in a) embankment bodies and b) foundation soils, for each analysed case study. Cross markers represent the median values of the distributions, solid lines the corresponding standard deviation error bars. In a) blue cross marker (Chisola SX embankment) is partially hidden behind green cross marker (Chisola DX embankment) due to their similar properties. c) Shift directions (indicated with arrows) between median V_s - R values of embankment body and foundation soils for each analysed case study.

4.1 Soil Type identification

Theoretical and statistical approaches allow the determination of the soil type. Soil type determination from geophysical data was therefore attempted in the investigated sites with these two methodologies (Fig. 5). With the statistical approach the soil is discretised in three classes: clay, sand and gravel with S_i values (Equation 9) ranging from 1 (clay) to 3 (gravel). In Figure 5a and 5b, the bounds between clay, sand and gravel, defined by the two black dashed lines, are reported. They were drawn by assuming Equation 9 respectively equal to 1.5 (boundary between clay and sand) and 2.5 (boundary between sand and gravel). Analogously, theoretical fine content fraction (C) curves (Figures 5c and 5d) were drawn following the methodology described in Section 3.1, assuming the clay resistivity, R_{clay} , as the minimum measured resistivity value for the given dataset and the fluid resistivity, R_f , on the basis of apriori information. The fine content fraction (C) doesn't provide by itself a clear identification of the soil type: however, many classifications available in scientific literature, are based (among other geotechnical parameters) on this parameter. As an example, the standard UNI EN ISO 14688-1:2018 (CEN 2018) identifies the fine content equals to 35% as the boundary between clayey sand and silt. From 35% up to 100%, the soil is classified into soft silt, soft clay, stiff clay and organic clay. The recommended soil for embankment construction falls into this group. By decreasing the fine content, clayey and silty sand, fine sand and gravel can be identified.

Cross-plots of R and V_s superimposed on the above defined limiting curves show that for both the analysed approaches, R - V_s values for embankment body (Figures 5a and 5c) mainly fall into the sand-clay domain. Conversely, foundation soils (Figures 5b and 5d) are classified as sand and gravel. The statistical approach tends to partially overestimate the soil type granulometry especially in foundation soils (Figures 5b and 5d) compared to the theoretical one. As an example, the foundation soil of Arignano earth dam, that is totally constituted of clay (Figure 2), was predicted to be sand. Similarly, constituting soil of Briaglia earth dam foundation was predicted to be gravel instead of clayey sand.

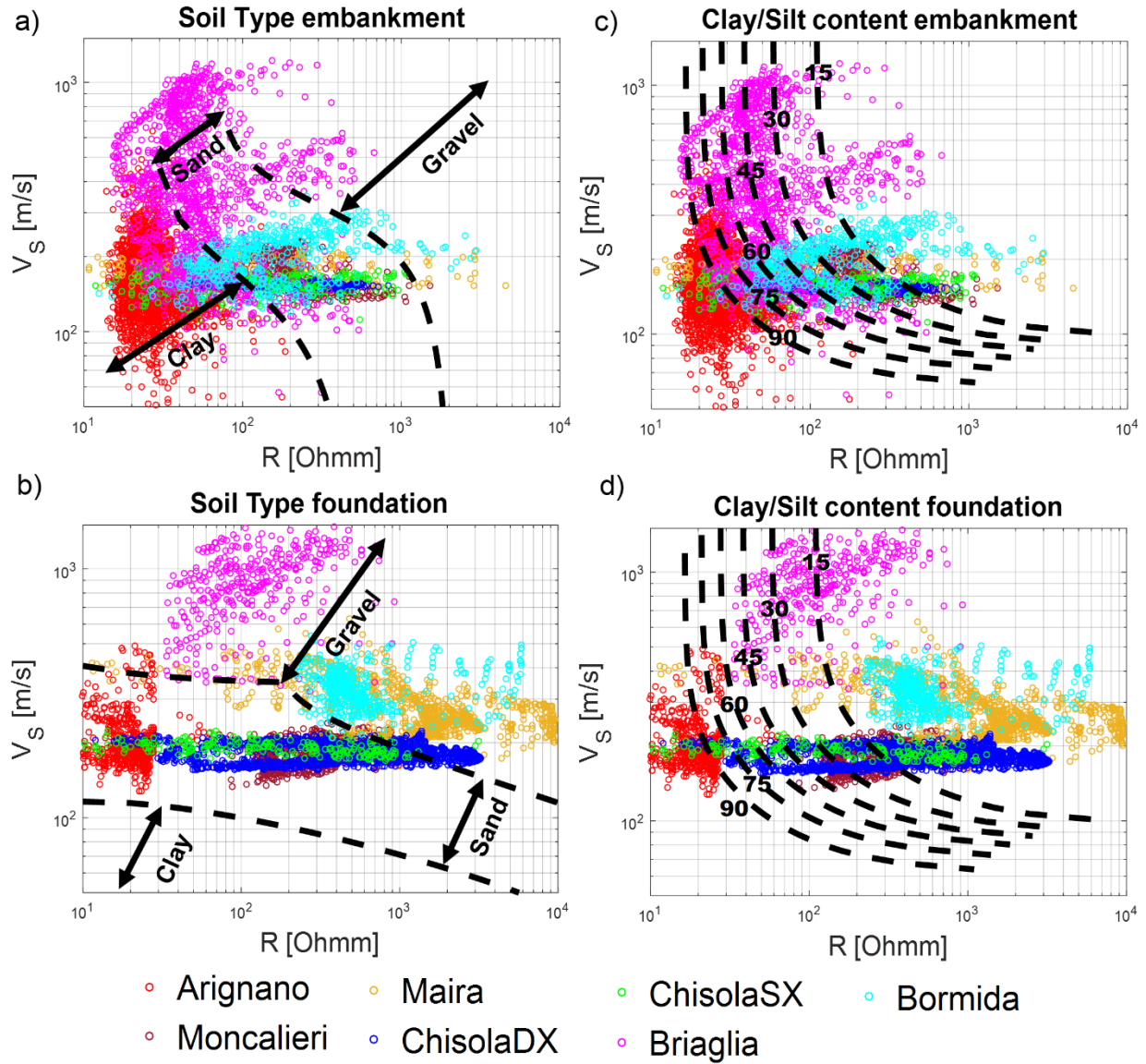


Figure 5. Soil classification as a function of shear wave velocity (V_s) and electrical resistivity (R) values based on a-b) Hayashi et al. (2013) approach and c-d) theoretical approach (Takahashi et al. 2014; Vagnon et al. 2021) for embankment bodies and foundation soils. In all the plots both the limits among different soil types from the proposed formulations (black dashed lines) and the experimental data measured in each test sites (coloured circles) are reported.

In order to quantitatively evaluate the differences between the two methods and evaluate the reliability in forecasting soil characteristics, the distributions of the fine fraction contents F_c and C derived by the statistical and theoretical methods, respectively, were evaluated along the longitudinal sections of each case study (Fig. 6). Normalised differences, defined as the ratio of the F_c - C difference to F_c , were also evaluated.

The two methods provide analogous results when the constituting soil is coarser and the percentage of sand and gravel is significant (Chisola SX, Chisola DX and Bormida embankment bodies and Maira and Bormida foundations, see also Fig. 2). Conversely, in embankments mainly constituted by clays and silts, the statistical approach generally underestimates the fine content. For instance,

analysing the data from the Arignano earth dam, F_c reaches values up to 60-70%, significantly smaller than those obtained by average grain size distributions (Fig. 2). The same considerations can be made for Moncalieri and Maira embankments where fine fraction reaches 75%: barring the first meter depth where the presence of road surfacing, with coarser soil, is well identified, the clayey and silty bodies are not satisfactorily recognized by this methodology. Moreover, the method is not sensitive to sharp soil variations. By focusing on Chisola SX embankment, the statistical approach forecasts a uniform F_c distribution, which is not representative of the real setting of the embankment since the soil in correspondence of the rebuilt sector (between 40 to 80 m) is more clayey than the surrounding original embankment body. Conversely, the theoretical approach is more versatile and faithfully forecasts the observed soil distributions. Sharp variations, both vertically, between embankment body and foundations and longitudinally, within the main bodies, are satisfactorily reproduced. Moreover, there is a general better correspondence among the observed C values and the ones expected on the basis of the geotechnical surveys.

The predicting capability of the two previous approaches was quantitatively evaluated by comparing the predicted F_c and C results with available grain size distributions performed on borehole logs. Results are listed in Table 2. Local investigations confirm that the forecasting capability of the statistical approach is effective when the constitutive soil is coarser (such as within the main body of Bormida embankment). For clayey and silty soils, the statistical approach generally underestimates the fine fraction content up to 70%, less than what observed in borehole logs. Conversely, the theoretical approach has a higher predicting capability, independently by the overall soil characteristics of the retaining structure with average differences of 15% with respect to borehole logs.

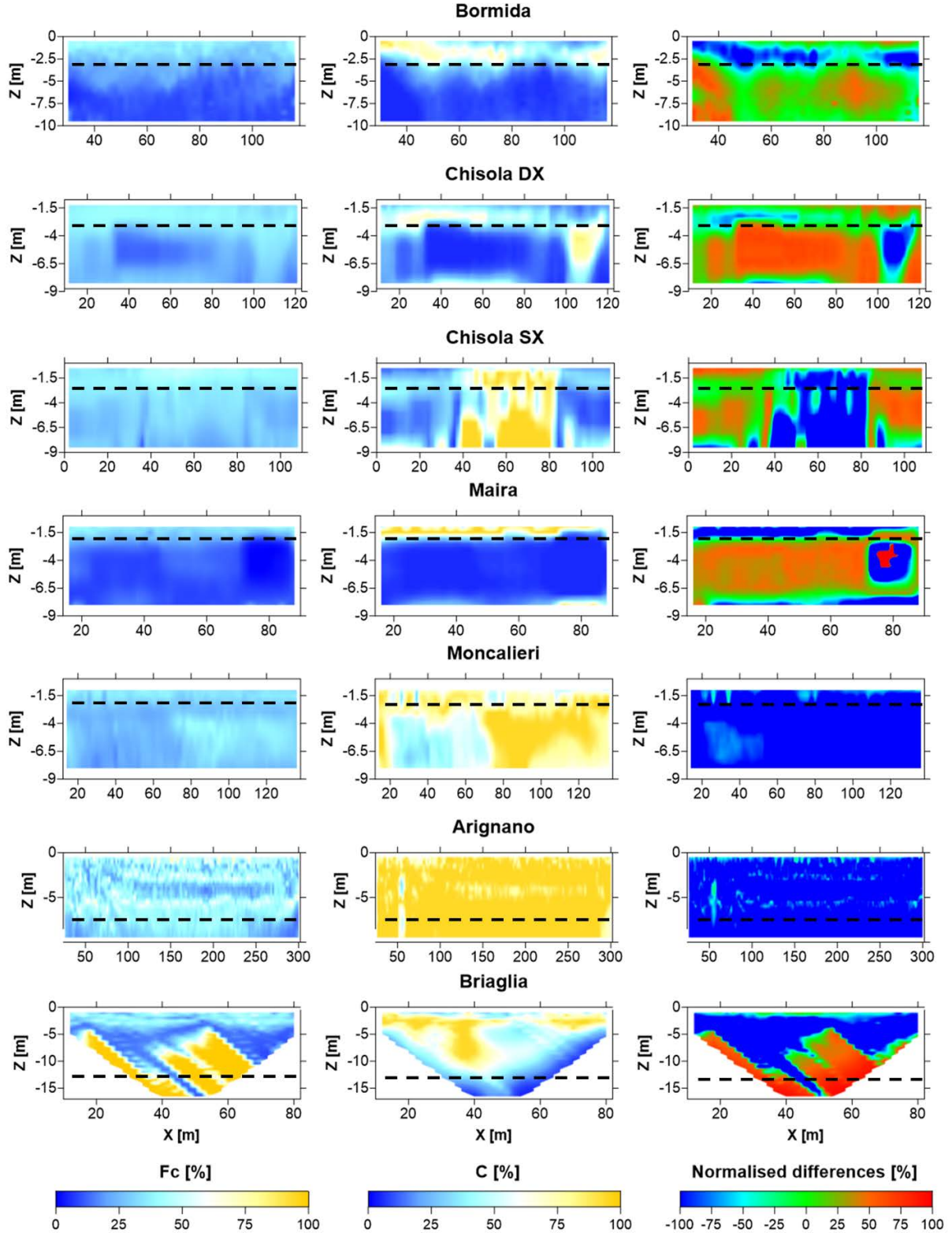


Figure 6. Distributions of fine fraction contents F_c and C derived by the statistical and theoretical methods and their respective normalised differences for each analysed case study. In each plot black dashed lines identify the transition from the embankment body to foundation soil.

Table 2. Comparison between fine fraction contents Fc and C derived by the statistical and theoretical methods and available grain size distribution from samples obtained in borehole logs at each test site.

	X [m]	Z [m]	Fc (<0.075m m) from boreholes [%]	Fc from statistical method (Hayashi et al. 2013) [%]	Difference [%]	C from theoretical method (Takahashi et al. 2014, Vagnon et al. 2021) [%]	Difference [%]
Bormida	48	4.8 - 5	87.6	20.95	76.08	25.00	71.46
		7 - 7.2	11.72	10.75	8.27	10.50	10.41
		8 - 8.2	9.72	9.72	0.02	10.00	-2.88
		9 - 9.3	2.21	9.40	-325.20	10.00	-352.49
Chisola SX	60	1	85.9	45.44	47.11	87.00	-1.28
	70	1	86.3	42.90	50.29	95.00	-10.08
	84	1	54.3	40.34	25.71	57.00	-4.97
Maira	14	1	77.41	24.86	67.89	7.33	90.53
	45	1	73.19	35.23	51.87	76.50	-4.52
	90	1	72.61	42.08	42.05	71.67	1.30
Briaglia	50	3 - 3.5	68	17.50	74.27	56.50	16.91
		15.5 - 16	65	10.65	83.61	43.00	33.85
Arignano	85	3.5 - 4	91.64	39.13	57.30	93.25	-1.76
		6.5 - 7	86.51	35.49	58.97	95.00	-9.81
	283	3.5 - 4	88.07	35.03	60.23	93.00	-5.60
		6.5 - 7	90.52	44.90	50.40	95.00	-4.95

4.2 Seepage index and hydraulic conductivity estimation

In Fig. 7 the seepage index, F, and hydraulic conductivity, K, distributions for each case study are shown. F and K are intimately linked each other since they provide information on embankment hydraulic conditions and possible sectors prone to piping and seepage phenomena.

As suggested by Chen et al. (2006), the empirical coefficients k_s and k_R depend on the overall geophysical and geotechnical conditions and they may in turn be calibrated on V_s and R distributions. In this study, since no evidence of seepage phenomena were previously detected, k_s and k_R were evaluated on the basis of the minimum V_s and R values observed in the surveys.

The values estimated for k_s and k_R in each test site are reported in Table 3.

The left column of Fig. 7 shows portions of the embankments with forecasted F values higher than 2 (yellow colour). In these portions there are no matches with previous geotechnical investigations of potential seepage phenomena. However, some of the reported high F values are located at the interface between embankment body and foundation (e.g Moncalieri, Maira, Chisola DX and Bormida), therefore from a theoretical point of view, their susceptibility to seepage and piping may be considered moderate to high. Conversely, Chisola SX embankment exhibits high F values ($F > 2$) in correspondence of the restored portion of the levee. In this sector, compacted clays were used as construction material. Seepage susceptibility may be expected at the interface between

natural and restored soil but hopefully not within the latter. Therefore in this situation the field-based approach fails in identifying a strong variation in material properties attributing the R and Vs variations to potential piping effects not reflecting the real state of the embankment. Contrary to the field-based approach, the theoretical approach allows the detection of sharp variations of K (right column of Fig. 7), with the main advantage of a rapid identification of the interfaces between soil with different hydraulic and geotechnical features. For instance, the presence of the brick channel along the Arignano dam (at about 50 m in longitudinal direction and at 3 m depth) is detected as a sector of high hydraulic conductivity compared to the surrounded clayey and silty soil with very low K values. This hydraulic contrast may be responsible of potential seepage and piping around the channel. The corresponding F distribution in this test site doesn't highlight this possibility (no F values higher than 2 are forecasted around the channel). Analogous observations can be extended to Chisola SX embankment where the restored soil is detected as a sector with very low K values, accordingly to the design material used during restoration works.

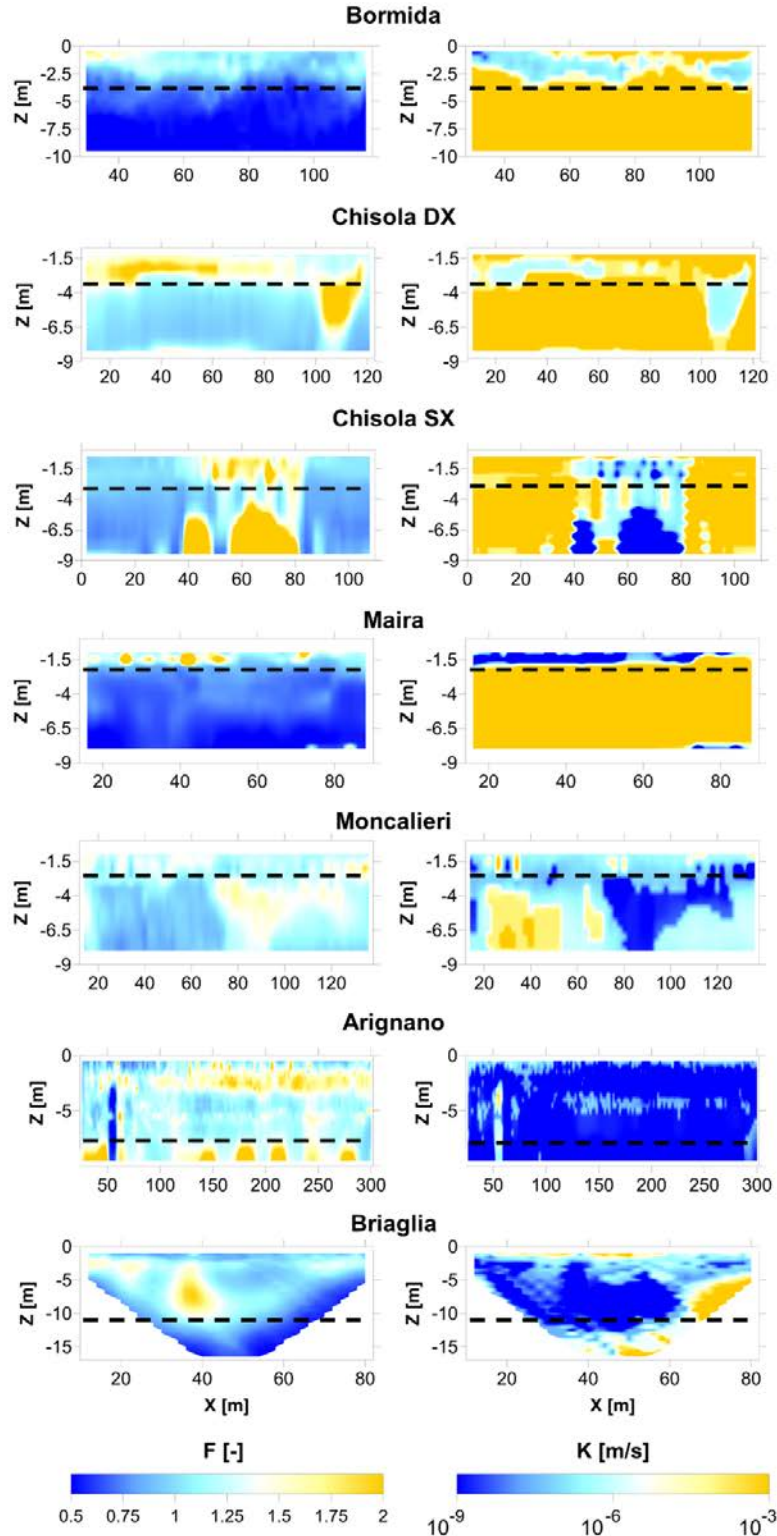


Figure 7. Distributions of the seepage index F (left columns) and the hydraulic conductivity K (right columns) for each analysed case study. In each plot black dashed lines identify the transition from the embankment body to foundation soil.

Table 3. List of k_S and k_R used for the evaluation of the seepage index F for each case study.

Site	k_S [m/s]	k_R [Ωm]
Bormida	145	22
Chisola DX	172	47
Chisola SX	136	19
Maira	165	11
Moncalieri	150	79
Arignano	50	24
Briaglia	49	25

5. Discussions

From the results reported in the paper it was observed that integrated seismic and electrical methods can be considered potentially useful tools for the characterisation of soil layering and related geotechnical parameters since they can be linked to soils stiffness (seismic properties) and water and clay content (electric properties), allowing for a preliminary classification as a function of soil fraction and providing indirect correlations with other important geotechnical parameters (e.g. hydraulic conductivity).

Notwithstanding this potentiality, some differences were observed in the obtainable results among the different adopted approaches, in comparison with available borehole data. The statistical approach discrepancies between predicted and observed fine fraction values can be related to the empirical and site-specific nature of this formulation. In fact, it was developed from measurements performed on Japanese earth retaining structures that might be slightly different, both in terms of geological and geotechnical features, from the embankments analysed in this work. Consequently, a devoted calibration of the polynomial coefficients in its formulation should be performed for optimizing the fit between estimated and observed parameters. For this calibration, however, a relevant number of independent geotechnical data and several case histories would be required.

On the contrary, the theoretical approach has a universal application, but it might be limited due to numerous assumptions necessary with respect to the parameters inherent in its formulation (such as clay and sand resistivity, interstitial water resistivity, critical porosity, saturation degree, etc.). At the same time, this approach allows punctual calibration with geotechnical observations, even if available in a limited number, for a detailed profiling of the retaining structure.

Apart from the limitations due to the soil characteristic assumptions, the main advantage of the theoretical model is its versatility since it can be employed in different saturation and soil conditions. Moreover, this approach also considers the confinement and the soil layering (in terms of depth and soil density). If borehole logs are available, the theoretical approach can be calibrated for estimating both the fine fraction content, C , and the hydraulic conductivity, K , distributions; on the other hand, it can forecast their distributions based on average reliable parameters.

Particularly, the possibility of estimating the hydraulic conductivity distribution along an earth retaining structure from geophysical data is fascinating. It must be however underlined that several constituting properties of the clay particles, such as its mineralogy and cation exchange capacity, are not explicitly considered in the theoretical formulation. These properties have been shown to have a paramount importance in the resulting hydraulic conductivity (e.g. [Revil et al. 1999](#)). With this respect, the electrical resistivity alone cannot be considered as an exhaustive parameter since electrical resistivity depends on both electrolytic conduction (fluid saturation and ionic composition) and surface conduction (in presence of clay particles or organic matter). The

contributions of these two entities are not easily distinguishable in survey results from the only resistivity. Indeed, the conduction mechanisms from soil surface charge are usually mainly associated to Induced Polarisation (IP). Several applications of IP surveys to the characterization of dams and river embankments can be found in literature (e.g. [Abdulsamad et al. 2019](#); [Soueid et al. 2020](#)) exploiting this technique for a more comprehensive characterization.

Nevertheless, the electrical resistivity measurements are still often adopted as a first characterization tool since their execution is significantly less time consuming than IP. Performing IP measurements with the same instrumentation adopted in the paper would indeed require longer current injection times, strongly increasing the survey time. In the aims of the present work, this is considered as a drawback since the study was focused on providing fast characterization tools for a first screening of the investigated structures. Further detailed characterization with geotechnical tests and/or with the same IP measurements will be required, particularly in correspondence of the location of the detected anomalies.

With this respect the provided hydraulic conductivity distributions must be considered more as a tool for identifying anomalous zones within the embankments than as an attempt to strictly quantify the hydraulic properties. In comparison with the empirical approach through the seepage index F , developed for the same aim, again the theoretical approach showed increased correspondence with available observations and a more comprehensive characterization at the different test sites reported in this paper. Particularly, at the Arignano earth dam, independent tests were performed to locally estimate the hydraulic conductivity (i.e. both variable-head hydraulic conductivity tests and laboratory oedometer tests). The results of these tests were observed to be in very good agreement with the ones from the distributions evaluated through the theoretical approach, with hydraulic conductivity values always within the same order of magnitude ([Vagnon et al. 2021](#)).

6. Conclusions

The comparison between the analysed procedures for geotechnical parameters estimation through electric and seismic data focused on strongpoints and limitations in forecasting earth structures characteristics in comparison with previously available geotechnical investigations.

The electric and seismic streamer surveys and the analysed methods for geotechnical profiling represent a good compromise between quality of the estimated data, costs and surveying time. The theoretical approach, notwithstanding the limitations inherent in the calibrating parameter necessary for its formulation, proved to be more effective in geotechnical estimation of the main earth retaining structure properties. However, all the described methodologies are thought for a first screening of earth retaining structures: consequently, independent geotechnical investigations are essential for calibrating and validating obtained results. Whenever direct geotechnical data are available at some profiles along the retaining structure, geophysical models should be properly calibrated and can then be used to extend punctual direct information to the whole structure. Once relevant anomalies are identified along the investigated structures with the proposed methods more detailed geophysical investigations (e.g. Induced Polarization measurements) or direct geotechnical investigations are necessary to allow a more precise definition of the geotechnical parameters of interest.

Acknowledgements

This work has been partially funded by FINPIEMONTE within the POR FESR 14/20 “Poli di Innovazione - Agenda Strategica di Ricerca 2016 – Linea B” call for the project Mon.A.L.I.S.A.

(313-67). Authors are gratefully to Daniele Negri for his fundamental help during acquisition surveys. Authors are also indebted with the Torino-Moncalieri AIPO division, and related personnel, for access permissions and for sharing information about the studied embankments.

References

Abdulsamad, F., Revil, A., Soueid Ahmed, A., Coperey, A., Karaoulis, M., Nicaise, S., Peyras, L., 2019. Induced polarization tomography applied to the detection and the monitoring of leaks in embankments. *Eng. Geol.* 254, 89–101.

Al-Fares, W., 2014. Application of electrical resistivity tomography technique for characterizing leakage problem in Abu Baara earth dam, Syria. *Int. J. Geophys.* 2014. <https://doi.org/10.1155/2014/368128>

Arato, A., Vagnon, F., Comina, C. 2021. A new seismo-electric streamer for combined resistivity and seismic measurements along linearly extended earth structures. *Geophys. J. Int.* (accepted after minor revision)

Arosio, D., Munda, S., Tresoldi, G., Papini, M., Longoni, L., Zanzi, L., 2017. A customized resistivity system for monitoring saturation and seepage in earthen levees: Installation and validation. *Open Geosci.* 9, 457–467. <https://doi.org/10.1515/geo-2017-0035>

Bièvre, G., Lacroix, P., Oxarango, L., Goutaland, D., Monnot, G., Fargier, Y., 2017. Integration of geotechnical and geophysical techniques for the characterization of a small earth-filled canal dyke and the localization of water leakage. *J. Appl. Geophys.* 139, 1–15. <https://doi.org/10.1016/j.jappgeo.2017.02.002>

Brovelli, A., and Cassiani, G. 2010. A combination of the Hashin-Shtrikman bounds aimed at modelling electrical conductivity and permittivity of variably saturated porous media. *Geophys. J. Int.* 180(1), 225–237.

Brown, W.A., Cegon, A.B., Sheng, Z., 2011. Utilizing continuous resistivity profiling for characterization of canal seepage in El Paso, Texas, in: *Proceedings of the Symposium on the Application of Geophysics to Engineering and Environmental Problems, SAGEEP*. pp. 169–178. <https://doi.org/10.4133/1.3614288>

Camarero, P.L., Moreira, C.A., Pereira, H.G., 2019. Analysis of the Physical Integrity of Earth Dams from Electrical Resistivity Tomography (ERT) in Brazil. *Pure Appl. Geophys.* 176, 5363–5375. <https://doi.org/10.1007/s00024-019-02271-8>

Carcione, J.M., Ursin, B., Nordskag, J.I., 2007. Cross-property relations between electrical conductivity and the seismic velocity of rocks. *Geophysics* 72. <https://doi.org/10.1190/1.2762224>

Cardarelli, E., Cercato, M., De Donno, G., 2014. Characterization of an earth-filled dam through the combined use of electrical resistivity tomography, P- and SH-wave seismic tomography

and surface wave data. *J. Appl. Geophys.* 106, 87–95.
<https://doi.org/10.1016/j.jappgeo.2014.04.007>

Carman, P.C. 1956. Flow of gases through porous media. Academic Press Inc.

CEN 2018. Geotechnical investigation and testing - Identification and classification of soil - Part 1: Identification and description. EN ISO 14688-1:2018.

Chen, C., Liu, J., Xia, J., Li, Z., 2006. Integrated geophysical techniques in detecting hidden dangers in river embankments. *J. Environ. Eng. Geophys.* 11, 83–94.
<https://doi.org/10.2113/JEEG11.2.83>

Comina, C., Vagnon, F., Arato, A., Fantini, F., Naldi, M., 2020a. A new electric streamer for the characterization of river embankments. *Eng. Geol.* 276.
<https://doi.org/10.1016/j.enggeo.2020.105770>

Comina, C., Vagnon, F., Arato, A., Antonietti, A., 2020b. Effective Vs and Vp characterization from Surface Waves streamer data along river embankments. *J. Appl. Geophys.* 183.
<https://doi.org/10.1016/j.jappgeo.2020.104221>

Cosentini, R.M., Foti, S., 2014. Evaluation of porosity and degree of saturation from seismic and electrical data. *Geotechnique* 64, 278–286. <https://doi.org/10.1680/geot.13.P.075>

Dabas, M., 2008. Theory and practice of the new fast electrical imaging system ARP©, in: *Seeing the Unseen: Geophysics and Landscape Archaeology*. pp. 105–126.
<https://doi.org/10.1201/9780203889558.ch5>

De Domenico, D., Garilli, G., Teramo, A., Marino, A., 2016. Application for capacitively coupled resistivity surveys in the city of messina, in: *22nd European Meeting of Environmental and Engineering Geophysics, Near Surface Geoscience 2016*.
<https://doi.org/10.3997/2214-4609.201601963>

Glover, P.W.J., Hole, M.J., Pous, J., 2000. A modified Archie’s law for two conducting phases. *Earth Planet. Sci. Lett.* 180, 369–383. [https://doi.org/10.1016/S0012-821X\(00\)00168-0](https://doi.org/10.1016/S0012-821X(00)00168-0)

Goff, D.S., Lorenzo, J.M., Hayashi, K., 2015. Resistivity and shear wave velocity as a predictive tool of sediment type in coastal levee foundation soils, in: *28th Symposium on the Application of Geophysics to Engineering and Environmental Problems 2015, SAGEEP 2015*. pp. 145–154. <https://doi.org/10.4133/sageep.28-026>

Hayashi, K., Inazaki, T., Kitao, K., Kita, T., 2013. Statistical estimation of geotechnical soil parameters in terms of cross-plots of S-wave velocity and resistivity in Japanese levees, in: *Society of Exploration Geophysicists International Exposition and 83rd Annual Meeting, SEG 2013: Expanding Geophysical Frontiers*. pp. 1259–1263.
<https://doi.org/10.1190/segam2013-0642.1>

635 Hashin, Z., and Shtrikman, S. (1963). "A variational approach to the theory of the elastic
636 behaviour of multiphase materials." *Journal of the Mechanics and Physics of Solids*, 11(2),
637 127–140.

638 Hoyois, P., Guha-Sapir, D., 2003. Three decades of floods in Europe: A preliminary analysis of
639 EMDAT data. Draft 1–15.

640 Kuras, O., Meldrum, P.I., Beamish, D., Ogilvy, R.D., Lala, D., 2007. Capacitive resistivity
641 imaging with towed arrays. *J. Environ. Eng. Geophys.* 12, 267–279.
642 <https://doi.org/10.2113/JEEG12.3.267>

643 Loke, M.H., Barker, R.D., 1996. Rapid least-squares inversion of apparent resistivity
644 pseudosections by a quasi-Newton method. *Geophys. Prospect.* 44, 131–152.
645 <https://doi.org/10.1111/j.1365-2478.1996.tb00142.x>

646 Mavko, G., Mukerji, T., Dvorkin, J., 2009. *The Rock Physics Handbook*, 2nd edition.
647 <https://doi.org/10.1017/cbo9780511626753>

648 Revil, A., et Cathles, L.M., Permeability of shaly sands, *Water Resources Research*, 35(3), 651-
649 662, 1999.

650 Rittgers J. B., A. Revil M. A. Mooney, M. Karaoulis, L. Wodajo, and C J. Hickey, 2016, Time-
651 lapse joint inversion with automatic joint constraints, *Geophysical Journal International.*,
652 207(3), 1401-1419,

653 Sørensen, K., 1996. Pulled array continuous electrical profiling. *First Break* 14, 85–90.
654 <https://doi.org/10.4133/1.2922124>

655 Soueid Ahmed, A., Revil, A., Abdulsamad, F., Steck, B., Vergnault, C., Guihard, V., 2020a.
656 Induced polarization as a tool to non-intrusively characterize embankment hydraulic
657 properties. *Eng. Geol.* 271.

658 Takahashi, T., Aizawa, T., Murata, K., Nishio, H., Consultants, S., Matsuoka, T., 2014. Soil
659 permeability profiling on a river embankment using integrated geophysical data, in: *Society
660 of Exploration Geophysicists International Exposition and 84th Annual Meeting SEG 2014.*
661 pp. 4534–4538. <https://doi.org/10.1190/segam2014-0620.1>

662 Vagnon, F., Comina, C., Arato, A., Chiappone, A., Cosentini, R.M., Foti, S. 2021. Geotechnical
663 screening of linear earth structures: electric and seismic streamers data for hydraulic
664 conductivity assessment of the Arignano earth dam. *J. of Geotech. and Geoenv. Eng.*
665 (accepted after major revision)

666 Weller, A., Lewis, R., Canh, T., Möller, M., Scholz, B., 2014. Geotechnical and geophysical
667 long-term monitoring at a levee of red river in vietnam. *J. Environ. Eng. Geophys.* 19, 183–
668 192. <https://doi.org/10.2113/JEEG19.3.183>